The stress-strain response curves for plain NC and SCC specimens and concrete-filled FRP composite specimens are plotted in Fig. 10, in which the first region of the axial stress-strain response of the composite cylinders coincides with the unconfined concrete response in both cases (NC and SCC-filled FRP tubes). For the same axial deformation value, the higher axial stress obtained in the case of SCC-FRP composite is attributed to the fact that the 91-day compressive strength of plain SCC is slightly higher than that of plain NC. For the axial stress-circumferential strain curves, Fig. 10 shows that the stiffness of the unconfined cylinders is slightly higher than that of the confined ones in both NC and SCC members. This behavior is likely due to the fact that the axial load was applied to the entire cross-section of the composite cylinder, and because concrete is stiffer than FRP, a higher value of circumferential strain is introduced at the outside surface of the FRP tube under the same axial load. The effect of using expansive cement instead of OPC in NC and SCC is demonstrated in Figs. 11 and 12 in which no significant change was observed in the confinement effect on concrete strength and ductility under uniaxial compression. Again the higher stresses in the response curves of NCE (normal concrete with expansive cement) are attributed to the fact that the unconfined compressive strength of NCE was slightly larger than that of the unconfined compressive strength of NC.

Flexural Test

The load-deflection curves of concrete-filled FRP composite tubes subjected to transverse load can also be characterized by three different regions, as it is the case for concrete-filled FRP tubes under uniaxial compression. However, the strength and stiffness of the FRP material dominated the behavior of such beam specimens during the loading process in all three stages. Since no steel was used to reinforce the concrete core in the unconfined beam specimens, their ability to carry transverse load was almost negligible. However, in the case of concrete-filled FRP composite beams, the concrete core contributed substantially to the overall strength and ductility of the composite specimens. Figs. 12 and 13 illustrate the load-deflection responses of confined and unconfined NC and SCC specimens along with the response of a hollow FRP tube, all subjected to transversal load. It is shown that the capacity of the FRP tube in sustaining transverse load increased by 175 % from 45 kN (ultimate load of hollow tube) to 124 kN (ultimate load of concrete-FRP composite member) and the maximum deflection of the tube at mid-span was also increased by 133 % from 21 mm in the case of a hollow tube to 49 mm in the case of an FRP-concrete composite beam. SCC specimens behaved relatively in a similar manner to

NC specimens and no major differences were observed during the loading process. Fig. 13 provides a comparison between the behavior of NC and SCC specimens under transverse load.

Slippage between the concrete core and the FRP tube may compromise the ultimate load capacity of the composite member, especially under transverse load. Therefore, an attempt was made to strengthen the interfacial bond between the two materials using expansive cement instead of OPC with the addition of a shrinkage-reducing admixture. This type of concrete will expand rather than shrink and therefore can create an active hoop pressure against the internal wall of the FRP tubes, therefore developing a better bond between the concrete core and the confining tube. Since such composite tubes are usually intended for use underground (saturated soil), subsequent shrinkage is considered less significant. The shrinkage-reducing admixture will reduce shrinkage strains, further enhancing this bond. The behavior of specimens prepared with such type of concrete is described in Figs. 13. It is shown that in the first and second stages of the response curve and at the same deformation, the load capacity of a GFRP tube filled with concrete using expansive cement is noticeably higher than that of a tube filled with concrete made of OPC, indicating that the specimen made with expansive cement was stiffer. However, the ultimate load and deflection of such specimens at failure was slightly lower than those of specimens made using OPC. This is believed to be due to the fact that the fibers in the FRP-concrete composite tube made using expansive cement were already prestressed due to the expansion of concrete before the loading process started.

Another attempt was made to prevent slippage by anchoring the FRP tube to concrete at 200 mm from each of its ends by inserting a 12-mm diameter steel bar in each of two holes drilled through the FRP before casting the concrete. It was later observed during testing that a local failure occurred in the concrete around the steel bars due to stress concentrations, and no major contribution to prevent slippage was noticed (Figs. 12). In fact, for all tested specimens slippage between the concrete and the FRP at both ends of each beam varied only between 1 mm and 3 mm. During the loading process, it was observed that each time slippage occurred between the concrete and the FRP, the load dropped, which explains the existence of harmonic events in the load-deflection curves of Figs. 12 and 13. All concrete-filled GFRP tubes shared the same failure mode. White lines along the fibers started to form at mid-span of the bottom section of the FRP tube and progressed towards the ends. Tensile cracks started to appear on the bottom section of the tube and under both loading points and progressed towards the upper section until a major crack was developed to cause a sudden failure as shown in Fig. 14.

CONCLUSIONS

This study investigated the behavior of concrete-filled GFRP tubes under both uniaxial compression and transverse loading for possible use in deep foundations (drilled-shaft piles). Special focus was on: i) the axial load-deformation response and axial stress-strain response of GFRP tubes filled with either NC or SCC under uniaxial compression; ii) the load-deformation behavior of such composite tubes under transverse load; and iii) the effect of using expansive cement and anti-shrinkage admixtures in concrete on the interfacial bond between the FRP tube and the concrete core. The following conclusions can be drawn from this investigation.

1. SCC-filled GFRP tubes had a similar behavior to that of NC filled-GFRP tubes under both uniaxial compression and transverse load.
2. The only significant difference between the behavior of NC and SCC-filled GFRP specimens was in the transition region of the response curves, in which the shift from a linear to a non-linear behavior in the load-deformation and stress-strain curves subsequent to the failure of the concrete core was more sudden for SCC-filled FRP specimens. This is believed to be due to autogenous and self-dessication shrinkage, which is higher in SCC due to a large volume of water and cement paste and lower volume of coarse aggregates. However, the use of expansive cement and shrinkage-reducing admixtures made the behavior of SCC-filled FRP tubes similar to that of NC-filled FRP tubes.
3. The use of expansive cement in concrete delayed the occurrence of slippage between the FRP tube and the concrete core, creating a somewhat better bond between the two materials, but did not fully prevent it. Likewise, the use of localized lateral steel bars placed through the FRP tube and concrete core did not prevent slippage. Shear connectors or ribs placed inside the FRP tubes may provide better performance (8).
4. FRP tube confinement of concrete cylinders increased their ultimate load by 2.5 times and their axial deformation by 12 times under uniaxial compression. It also enhanced their ultimate load by 20 times and their mid-span deflection by 100 times under transverse load.

REFERENCES

1. Sen, R., Shahawy, M., Rosas, J. and Sukumar, S., "*Durability of AFRP and CFRP Pretensioned Piles in Marine Environment,*" Non-Metallic (FRP) Reinforcement for Concrete Structures, Proceedings of the Third International Symposium, Vol. 2, 1997, pp. 123-130.

2. El-Nawawy, O. and Kandeil, A., "*A New Reinforcing Material for Concrete in the Arabian Gulf,*" Proceedings of the 2nd International Conference on Deterioration and Repair of Reinforced Concrete in the Arabian Gulf, CIRIA, Bahrain, 1987, pp. 185.

3. Mirmiran, A. and Shahawy, M., "*Behavior of Concrete Columns Confined by Fiber Composites,*" Journal of Structural Engineering, Vol. 123, No. 5, 1997, pp. 583-589.

4. Samaan, M. S., "*An Analytical and Experimental Investigation of Concrete-Filled Fiber Reinforced Plastics (FRP) Tubes,*" Ph.D. Thesis, University of Central Florida, Orlando, FL., 1997, 220 p.

5. Knowls, R. B., and Park, R., "*Strength of Concrete Filled Steel Tubular Columns*," ASCE, Journal of the Structural Division, Vol. 95, ST12, 1969, pp. 2565-2587.

6. Mander, J. B., Park, R., and Priestly, M. J. N., "Theoretical Stress-Strain Model for Confined Concrete," Journal of Structural Engineering, ASCE, 114 (8), 1988, pp. 1804-1826.

7. Samaan, M., Mirmiran, A. and Shahawy, M., "Model of Concrete Confined by Fiber Composites," Journal of Structural Engineering, Vol. 124, No. 9, 1998, pp. 1025-1031.

8. Mirmiran, A., Shahawy, M., Samaan, M., El Echary, H., Mastrapa, J. C., Pico, O., "*Effect of Colomun Parameters on FRP-Confined Concrete,*" Journal of Composites for Construction, Vol. 2, No. 4, 1998, pp. 175-185.

NOTATIONS

α = Winding angle of glass fibers in the FRP tubes.
ν = Poisson ratio.
Δ_{co} = Maximum axial deflection of unconfined cylinders at concrete failure.
Δ_{cc} = Maximum axial deflection of confined cylinders at concrete failure.
Δ_{ult} = Ultimate axial deflection of confined cylinders at failure.
Δ_{max} = Maximum mid-span deflection of specimen subjected to pure bending.
ε_{co} = Maximum axial strain of unconfined cylinders.
ε_{cu} = Ultimate axial strain of confined cylinders.
ASHA = Anti-shrinkage admixtures.
C = Cement.
D = Inside diameter of FRP tubes.
E = Modulus of elasticity of FRP tubes.
EC = Expansive cement.
FA = Fly ash.
G = Gravel.
GBFS = Granulated blast furnace slag.
GFRP = Glass fiber-reinforced plastic.
L = length of specimen.
NC = Normal concrete.
NCE = Normal concrete with expansive cement and anti-shrinkage admixtures.
OPC = Ordinary portland cement.
P_{co} = Maximum axial load of unconfined cylinder at concrete failure.
P_{cc} = Maximum axial load of confined cylinder at concrete failure.
P_{ult} = Ultimate axial load of confined cylinder at failure.
P_{max} = Maximum transversal load of cylinder subjected to pure bending.
S = Sand.
SCC = Self-compacting concrete.
SCCE = Self-compacting concrete with expansive cement and anti-shrinkage admixtures
SP = Superplasticizer.
VMA = Viscosity-modifying admixtures.
W = Water.
W/C = water to cement ratio.
f'_c = Compressive strength of unconfined concrete specimen .
f'_{cu} = Ultimate compressive strength of confined concrete specimen .
t = Thickness of the FRP tube.

Table 1- Mixture proportions and compressive strengths of concrete batches

Mixtures	W/B[1]	Component (kg/m³)						SP[1] (L/m³)	VMA[1] (%)	ASHA[1] (L/m³)	f'_c (MPa)	
		W[1]	C[1]	FA[1]	GBFS[1]	S[1]	G[1]				28-d	90-d
NC[2]	0.45	160	355	-	-	700	1050	-	-	-	34.5	39.5
SCC[2]	0.45	180	200	80	120	850	850	2	0.04	-	35.5	43.8
NCE[2]	0.45	155	355	-	-	700	1050	-	-	4	37.0	42.0
SCCE[2]	0.45	180	200	80	120	850	850	2	0.04	4	38.5	45.4

[1, 2] See NOTATIONS.

Table 2- Physical and mechanical properties of FRP tubes

D* (mm)	t* (mm)	α*	Glass content (%)	Axial direction		Hoop direction		Poisson's ratio (ν)	
				Strength (MPa)	E * (GPa)	Strength (MPa)	E* (GPa)	Lateral / transverse	Transverse/ lateral
15.0	6.0	±55°	53.5	60.0	8.5	193.0	10.5	0.39	0.5

* See NOTATIONS.

Table 3- Properties of cylindrical specimens prepared for uniaxial compression

Cylinder's type	Concrete mixtures	f'_c (MPa)		No. of conf. cylinders	No. of unconf. cylinders	t[1] (mm)	D[1] (mm)	L[1] (mm)
		28- d	90-d					
NC	NC	34.5	39.5	2	2	6	150	300
SCC	SCC	35.5	43.8	2	2	6	150	300
NCE	NCE	37.0	42.0	2	-	6	150	300
SCCE	SCCE	38.5	45.4	2	-	6	150	300
FRP	Hollow	-	-	-	2	6	150	300

Table 4- Properties of cylindrical beam specimens prepared for flexural test

Cylinder's type	Concrete mixture	f'_c (MPa)		No. of conf. cylinders	No. of unconf. cylinders	t[1] (mm)	D[1] (mm)	L[1] (mm)
		28-d	90-d					
BNC	NC	34.5	39.5	2	2	6	150	1100
BSCC	SCC	35.5	43.8	2	2	6	150	1100
BNCE	NCE	37.0	42.0	2	-	6	150	1100
BSCCE	SCCE	38.5	45.4	2	-	6	150	1100
FRP	Hollow	-	-	-	2	6	150	1100

[1] see NOTATION.

Table 5- Test results for specimens subjected to uniaxial compression

Cylinder's type	P_{co}* (kN)	P_{cc}* (kN)	P_{ult}* (kN)	Δ_{co}* (mm)	Δ_{cc}* (mm)	Δ_{ult}* (mm)	f'cu* (MPa)	ε_{co}*	ε_{cu}*
NC	690	913	1770	1.59	1.38	19.0	85.8	0.005	0.06
SCC	774	1032	1736	1.50	1.35	16.4	84.2	0.005	0.05
NCE	-	1031	1743	-	1.58	16.7	84.5	-	0.05
SCCE	-	983	1784	-	1.53	20.0	86.5	-	0.06
FRP	-	-	420	-	-	7.4		-	0.02

*See NOTATIONS

Table 6- Test results for specimens subjected to transverse load

Cylinder's type	f'c (28-d) (MPa)	Unconfined specimens		Confined specimens	
		P_{max} (kN)	Δ_{max} (mm)	P_{max} (kN)	Δ_{max} (mm)
NC	34.5	6.5	0.45	124.0	49.7
SCC	35.5	6.1	0.45	121.5	50.0
NCE	37.0	-	-	118.5	39.0
SCCE	38.5	-	-	118.0	53.5
FRP	-	45.0	21.0	-	-

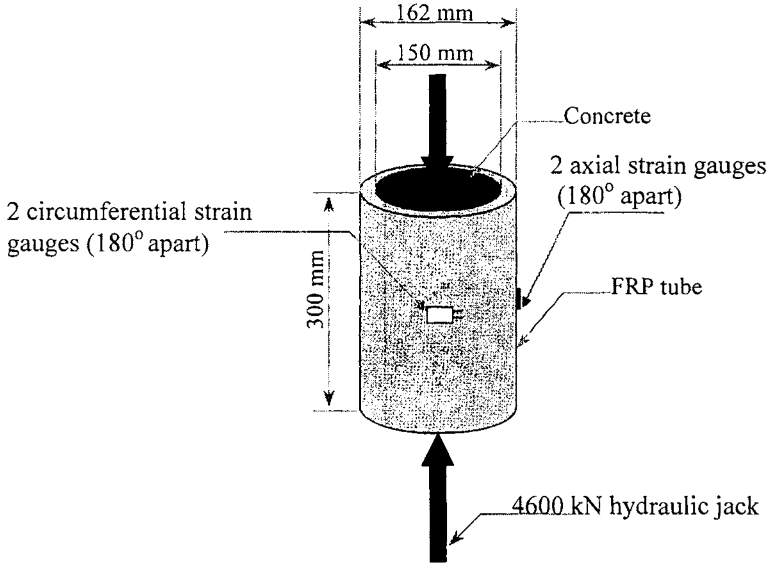

Fig. 1- Illustration of specimen used in uniaxial compression

Fig. 2- Test set-up for uniaxial compression.

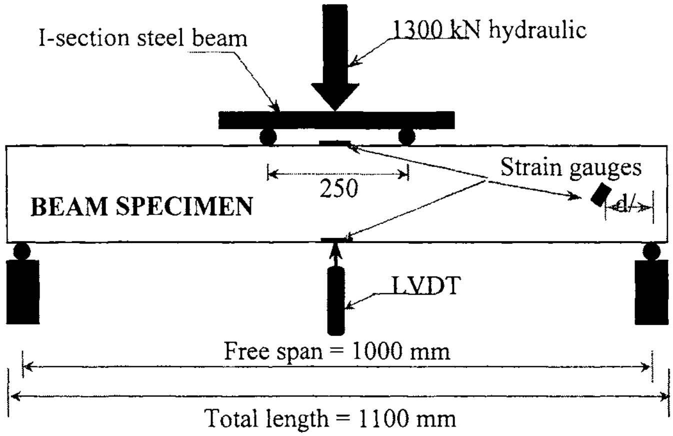

Fig. 3- Illustration of test specimen subjected to transverse load.

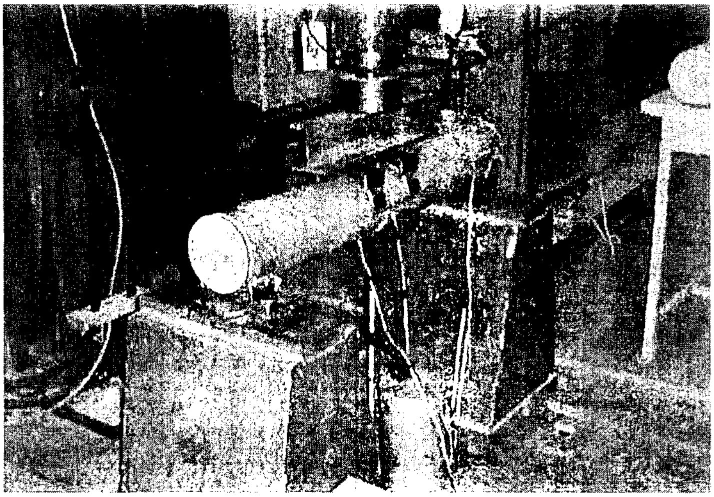

Fig. 4- Test set-up for flexural test.